Expert Opinion

The application of microbubbles for targeted drug delivery

Joseph L Bull
The University of Michigan, Departments of Biomedical Engineering and Surgery, Ann Arbor, MI 48109, USA

Interest in microbubbles as vehicles for drug delivery has grown in recent years, due in part to characteristics that make them well suited for this role and in part to the need the for localized delivery of drugs in a number of applications. Microbubbles are inherently small, allowing transvascular passage, they can be functionalized for targeted adhesion, and can be acoustically driven, which facilitates ultrasound detection, production of bioeffects and controlled release of the cargo. This article provides an overview of related microbubble biofluid mechanics and reviews recent developments in the application of microbubbles for targeted drug delivery. Additionally, related advances in non-bubble microparticles for drug delivery are briefly described in the context of targeted adhesion.

Keywords: cardiovascular fluid mechanics, contrast agent, interfacial flows, localized chemotherapy, microbubble, ultrasound

Expert Opin. Drug Deliv. (2007) 4(5):475-493

1. Introduction

Interest in microbubbles as suitable vehicles for drug delivery has grown in recent years. Blood-borne microbubbles are significant in a number of applications, such as ultrasound contrast agents, neovascularization and air embolism. Consequently, a number of recent reviews have considered a variety of applications of microbubbles [1-5]. This article aims to review recent developments in the application of microbubbles for targeted drug delivery and to provide an overview of related bubble dynamics. First, an introductory review of microbubble biofluid mechanics and the potential applications of microbubble drug carriers is presented. Subsequently, recent progress in microbubble carriers, targeting approaches, drug release dynamics and microbubble clearance are described. These sections also include a brief discussion of related work on drug delivery via microparticles without gas cores, focusing on targeting and encapsulation features that could potentially be incorporated into microbubble carriers. This is followed by a discussion of conclusions and future directions.

1.1 Microbubble and interfacial dynamics

The dynamics of microbubbles suspended in blood is governed by a complicated coupling between the mechanics of the gas comprising the bubble, the interface or shell encapsulating the bubble, and the surrounding blood. Understanding the resulting microbubble dynamics is paramount to developing sophisticated approaches to microbubble drug delivery. Gas transport, which is usually undesirable for microbubble drug carriers, into or out of the microbubble can be an additional complication.

1.1.1 Cardiovascular biofluid mechanics

Cardiovascular biofluid mechanics has been the topic of several reviews [6,7] and is only briefly reviewed here to provide a basis for discussing microbubble dynamics.

informa
healthcare

Although blood is a complex suspension of cellular components within plasma, there are many flow scenarios in which blood may be considered as a continuum due to the small size of cellular components compared with the vessel diameters. Plasma itself is a Newtonian fluid, meaning it exhibits a linear relationship between shear stress and strain rate [8,9], but the presence of cellular components result in blood's non-Newtonian behavior. Blood is visco-elastic, meaning that it behaves as a solid when the shear stress is below its yield stress, and behaves as a shear thinning fluid when shear stress exceeds the yield stress [8,9].

For small enough vessels, such as capillaries, whose diameters are similar to that of red blood cells, the continuum approximation of blood is not valid. Consequently, studies of small-scale blood flow have considered the transport and deformation of individual red blood cells suspended in plasma, rather than considering blood to be a homogenous continuum [10-16]. Previous studies of droplet suspensions have demonstrated that interfacial effects can lead to 'tank treading' and deformations of droplet shapes [10,12,17-25]. Red blood cells undergo a tank-treading motion of the cell membrane about the cell interior [26,27]. The part of the cell membrane near the vessel wall has small relative motion with respect to the wall and the part of the cell membrane closer to the center of the vessel moves forward. This reduces resistance to movement of the elongated cell in the vessel [9].

Blood flow is governed by conservation of fluid mass and conservation of linear momentum, which can be described mathematically by the continuity and Navier-Stokes equations for an incompressible, Newtonian fluid:

$$\nabla \cdot \vec{u} = 0 \tag{1}$$

$$\rho\left(\frac{\partial \vec{u}}{\partial t} + (\vec{u}\cdot\nabla)\,\vec{u}\right) = -\nabla p + \quad \nabla^2\vec{u} + \rho g\vec{e}_g \tag{2}$$

In this equation, ρ is fluid density, g is acceleration due to gravity, $\vec{e}_g$ is a unit vector in the direction of gravity, $\vec{x}$ is the position vector, $\vec{u}$ is the velocity vector, p is pressure, and μ is fluid viscosity. For non-Newtonian models of blood, the stress terms in the conservation of momentum equation reflect the stress–strain rate relationship for the fluid. The vessel wall conditions, the appropriate conditions on the blood entering and leaving the region of interest, and the presence of microbubbles dictate the appropriate boundary conditions on these governing equations. Analysis of physiologic cardiovascular flows can require appropriate simplifications and proper analysis requires retention of the dominant terms. Conservation of blood momentum and mass provide insights into the behavior of actual blood flow, and provide a basis for computational modeling of blood flow [6,7,28-38].

1.1.2 *Interfacial tension*

The gas comprising microbubbles is compressible, and is also subject to conservation of mass and momentum. The interfaces and encapsulating shells of microbubbles can deform. These deformations can be significant factors in the overall behavior of the microbubbles and in the generation of bioeffects in vessel walls near microbubbles. Interfacial tension is responsible for many commonly observed phenomena. Just a few examples include the break-up of jets into droplets (Rayleigh instability), the tendency of gas bubbles to assume a spherical shape in many equilibrium conditions, the rise of liquids in capillary tubes, and the formation of 'wine tears' on the inner surface of a wine glass (a thin layer of wine forms on the glass above the surface of the wine and droplets or 'tears' flow back into the wine, due to the effects of surface tension gradients, gravity and evaporation) [1,39-48]. Interfacial dynamics, which is described extensively elsewhere [47-52], is briefly summarized here.

The pressure jump, Δp, across a static interface is related to the mean interfacial curvature, κ_m and interfacial tension, σ, by the Young-Laplace law:

$$\Delta p = 2\sigma\kappa_m \tag{3}$$

This law indicates a larger jump in pressure for interfaces with a higher curvature or higher interfacial tension. More complicated constitutive equations can be used to account for interfacial viscosities and moduli of elasticity, and are described in detail elsewhere [47]. The more general form of Equation 3 that applies to a dynamic interface is:

$$\Delta\vec{f} = \sigma\kappa\hat{n} + \nabla_s\sigma \tag{4}$$

In this equation, f^{ω} is the traction at the interface, defined as $\vec{f} = \underline{\underline{\sigma}} \cdot \hat{n}$, $\underline{\underline{\sigma}}$ is the stress tensor, ∇_s is the surface gradient operator, $\hat{n}$ is the unit normal to the interface, and $\Delta\vec{f}$ is the jump in traction across the interface (e.g., the difference between the traction in the gas and traction in the blood). The stress tensor for a Newtonian fluid is:

$$\underline{\underline{\sigma}} = (-p - g\vec{e}_g \cdot \vec{X})\underline{\underline{I}} + \quad (\nabla\vec{u} + [\nabla\vec{u}]^T) \tag{5}$$

$\underline{\underline{I}}$ is the identity matrix. Thus, we can see that Equation 3 indicates that the normal stress jump is balanced by the interfacial curvature term and the jump in tangential stress is balanced by the interfacial tension gradient. In the absence of surfactants (surface active species) and temperature variations, σ is typically assumed constant. When surfactants are present, as can be the case in the blood and encapsulated microbubbles, σ depends on the interfacial surfactant concentration.

The interface moves with the same normal component of velocity as the fluid at the interface, known as the interfacial kinematic boundary condition, such that:

$$\frac{\partial \vec{Y}}{\partial t} \cdot \hat{n} = \vec{u} \cdot \hat{n} \quad (6)$$

$\vec{Y}$ is the interface position. The interfaces of microbubbles can deform with flow and acoustic driving, and consequently their shapes evolve in time. The evolution of microbubble interfaces and fluids (gas in the bubble and blood surrounding the bubble) are coupled, and theoretically predicting the microbubble behavior requires solving an inherently complex coupled moving boundary problem. Interfacial tension can significantly impact the stresses and velocities at interfaces, and is important in a wide variety of physiological flows [53-66].

1.1.3 *Gas transport*

In addition to deformation due to flow, interfacial tension, changes in surrounding blood pressure, and acoustic driving, microbubbles can grow or shrink as gas enters or leaves the microbubble. Blood-soluble gases are transported within the blood by convection and diffusion. Conservation of gas mass in the bulk yields the gas transport equation:

$$\frac{\partial C}{\partial t} + \nabla \cdot (C\vec{u}) = \nabla \cdot (D \nabla C) \quad (7)$$

C is the gas concentration in the blood and D is the gas diffusivity in blood. The Peclet number, $Pe = UL/D$, indicates the relative importance of convection compared with diffusion, where U is the characteristic velocity scale, and L is the characteristic length scale. As can be seen from Equation 7, convective gas transport in the blood is dependent on the velocity field in the blood. Thus, the tendency of microbubbles to grow or shrink can be significantly affected by blood flow, and static microbubbles are expected to deflate at a slower rate than freely circulating ones. Additionally, encapsulation of microbubbles can substantially slow diffusion of gas out of the microbubble. Transport of gas out of microbubbles and through the nearby blood can significantly affect microbubble stability, which is discussed below.

1.2 Potential applications

The effectiveness of chemotherapy, which is intended to eradicate rapidly proliferating cancer cells, is often hampered by the systemic toxicity of the chemotherapy agents. Thus, localized drug delivery could have a significant impact in improving the efficacy and minimizing the side effects associated with chemotherapy. For example, doxorubicin is a common chemotherapeutic because of its multiple modes of action, but its side effects, such as cardiotoxicity and nephrotoxicity, limit dosing and effectiveness [67,68]. Consequently, there is considerable interest in microbubbles for the localized delivery of chemotherapy agents. Additionally, localized delivery of drugs and genetic materials to atherosclerotic plaques, thrombus, and other regions of cardiovascular disease [18,69-73], as well as drug delivery to the brain [74], has attracted interest.

2. Microbubble carriers

2.1 Gas components

Microbubbles for drug delivery are similar in composition to microbubble contrast agents, which were developed to enhance the acoustic signal from blood during ultrasound imaging. First-generation ultrasound contrast agents were comprised of air [2,75-78]. As noted above, the transport of gas out of microbubbles is influenced by convection and diffusion. Many of these first-generation microbubble contrast agents had limited success. They were hindered by short circulation times that resulted from the gas comprising them being absorbed by the surrounding blood. In the 1990s, two primary approaches were taken to address this challenge of bubble stability: use of low-solubility gases (high molecular weights and low diffusivities) and thick gas impermeable shells for encapsulating the microbubbles. Subsequent microbubbles were engineered using one or a combination of these approaches. Most of these microbubbles have been comprised of air, nitrogen, perfluorocarbons, or sulfur hexafluoride [2,79-84].

2.2 Shell components

As noted above, bubble stability is a primary consideration in designing microbubbles. Prior to the second generation of microbubble contrast agents, the presence of surface-active lipids or proteins that form monolayers at the interface of gas bubbles had been demonstrated to stabilize bubbles in studies related to cavitation, decompression sickness and air embolism [85-91]. Although microbubble stabilization is undesired in air embolism, it is needed for effective ultrasound contrast agents. The encapsulation of microbubbles has resulted in significantly improved stability [85-103]. A schematic of a lipid-encapsulated microbubble, with ligands for targeted adhesion and the drug cargo incorporated into the shell, is shown in **Figure 1**.

A number of surface-active materials have been investigated for encapsulation of microbubble ultrasound contrast agents, including lipids [92,93,95,104-110], proteins and polymers [96,111-114]. An investigation of alginate encapsulation of genetically modified cells concluded that this approach may be an effective strategy for delivering therapeutics to the injured spinal cord [115]. The release of fluorescein isothiocyanate labeled bovine serum albumin from alginate-microencapsulated liposomes showed the potential of that system for drug delivery [116]. The development

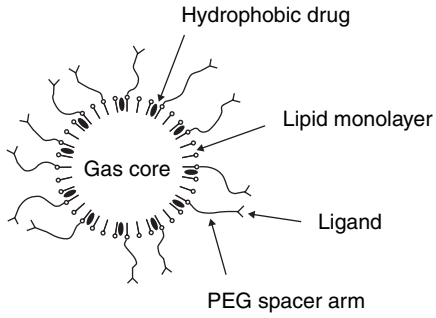

Figure 1. An encapsulated microbubble, with hydrophobic drug cargo incorporated into the lipid shell. PEG spacer arms connect the ligands to the shell.

of effective encapsulation approaches has resulted in transvascular microbubbles sufficiently stable for imaging and drug delivery. Just two examples of encapsulated microbubbles are Definity® (Bristol-Myers Squibb Medical Imaging) and Sonovist® (Schering AG), which use a lipid/surfactant shell and a cyanoacrylate polymer shell, respectively.

Microbubbles with surface-active coatings, such as lipids, are usually formed by high-shear dispersion of the core gas within aqueous media that contains the lipid in micellar or liposomal form. Such shear flows can arise from sonication or other scenarios [117,118]. When the gas is dispersed in the media, the surface-active lipids form a monolayer on the microbubble interface. The size distribution of the resulting microbubbles depends on the flow parameters, and the gas and lipid properties. Recent work has also used microfluidics circuits to produce encapsulated microbubbles [119]. The addition of a negatively charged lipid within the bulk lipid [120] or surface brush of a hydrophilic polymer, such as PEG [2], reduces the rate of shell fusion and microbubble coalescence. Commercially available microbubble contrast agents of this type are typically dry preparations that are reconstituted prior to injection and require use within hours after preparation [117,120]. More stable preparations (years of storage in the aqueous form) may be produced with thicker shells, such as denatured albumin [80], gel phase lipids with surface PEG brushes [121], or solid polymers [122], to avoid fusion. Despite this success in producing stable microbubbles for use as ultrasound contrast agents, microbubble stability is an important research topic, particularly as it relates to drug delivery. Unstable microbubbles could compromise the ability of these approaches to deliver drugs to the targeted location and could result in unintentional delivery to other tissues. Stronger shell components enhance stability but modify the acoustic response of the microbubble.

A number of studies have examined microbubble stability and the dynamics of the encapsulating lipid during microbubble dissolution. Borden and Longo [123] examined gas transport and dissolution of lipid-encapsulated microbubbles. They found gas permeation resistance to be a significant factor in controlling the dissolution rate of lipid-coated microbubbles and noted that it increased monotonically with lipid hydrophobic chain length. For short-chain lipids, the dissolution process involved continuous shedding of lipid from the shell to accommodate the bubble's shrinking gas volume. They observed a cyclic process of buckling and shedding of long-chain lipids and a proposed a mechanism involving adhesive zippering of apposing monolayers to describe the phenomenon.

In another study, Borden *et al.* used langmuir trough methods and fluorescence microscopy to investigate the phase behavior and microstructure of monolayer shells coating microbubbles [124]. The monolayer shells were composed of a homologous series of saturated acyl chain phospholipids and an emulsifier containing a single hydrophobic stearate chain and PEG head group. An assortment of condensed phase area fractions and domain morphologies were observed in each batch of microbubbles. Compression of the monolayer past the PEG-emulsifier squeeze-out surface pressure resulted in a dark shell composed entirely of lipid, and under certain conditions, the PEG-emulsifier was reincorporated upon subsequent expansion. A related investigation demonstrated a variety of lipid monolayer collapse modes during dissolution of encapsulated air microbubbles, including substantial surface buckling with simultaneous nucleation and growth of folds for very rigid monolayers [125]. A study of lipid-coated microbubble shells using a combination of spectroscopy and microscopy techniques found that the shell forms ordered domains that are composed primarily of phosphatidyl choline, and disordered interdomain regions that are enriched in lipopolymer [126]. The authors noted that the overall high variation in microstructure highlights the nonequilibrium (history-dependent) nature of the monolayer shell and that the surface distribution of the shell species dictates ligand location, brush coverage and amount of drug loading.

Other studies have examined the stability of microbubbles when exposed to ultrasound and found that i) higher concentrations of microbubbles, lower ultrasound transmit power settings, and intermittent imaging each can reduce the rate of destruction of microspheres [127]; and ii) the destruction of gas-filled microbubbles in the ultrasound field of the medical imaging system is influenced by the nature of the gas inside the bubbles with deflation occurring substantially faster for air-filled bubbles compared with perfluorocarbon-filled bubbles [128]. Lankford *et al.* investigated whether microbubble attachment to cells influences their acoustic signal generation and stability [129]. They concluded that attachment of targeted microbubbles to rigid surfaces results in damping and a reduction of their acoustic signal, which is not seen when microbubbles are attached to cells. They also demonstrated that that free microbubbles undergo a reduction in size and concentration after their removal from a gas-saturated environment and placement in room air-equilibrated culture medium at 37°C for 20 min. However, microbubble attachment to cells prevented gas

volume loss under the same conditions, perhaps due to differences in gas transport and bubble interface behavior.

In addition to the shell for encapsulation, microbubbles for targeted imaging or drug delivery often include other components, such as ligands for targeted binding and/or arms to which ligands are attached. Targeting approaches are described in more detail in Section 3. As discussed in more detail below, some microbubble carrier designs for drug delivery incorporate the drug cargo into the shell. Although microbubbles for drug delivery are similar those for ultrasound contrast, the addition of the drug cargo and consideration of optimal delivery may require modifications to optimize drug delivery. For example, surface distribution of the encapsulating shell species can affect ligand location, brush coverage, and amount of drug loading; and it has been shown that there is a high overall variation in microstructure, including the existence of anomalous three-phase coexistence, in lipid monolayer shells [126].

2.3 Carrier designs

Several approaches to microbubble carrier design have been explored in the literature [69,103,116,130-139]. These can be classified as i) co-administration; ii) attachment; iii) incorporation, and iv) containment [3]. In co-administration, the drug delivery vehicles are co-administered along with the microbubbles, but are separate from the microbubbles [137,139]. This approach makes use of the enhanced vessel wall permeability that can be induced by microbubbles, but does not require development of specific microbubble carriers. In attachment, the drug or drug delivery vehicles are attached to the microbubble shell. Incorporation refers to the drug or delivery vehicles being incorporated into the microbubble shell [140], as illustrated in **Figure 1**. In the containment approach, drug is contained within the mircobubble, rather than within the shell. The choice of design approach depends on the drug, gas, shell material, target site and targeting approach. For example, a surface-active monolayer shell with a water-soluble drug cargo inside the gas core of the bubble may not be a stable configuration [5]. A dry drug inside the bubble would absorb water in order to minimize the system's free energy, resulting in an unstable monolayer configuration. However, such a drug in a gas core contained within a solid polymer shell would be stable [5,141].

3. Targeting approaches

3.1 Specific ligands and targets

Targeted microbubbles are of interest for both therapeutic and diagnostic applications, and a number of targeting approaches have been investigated. Targeted adhesion of micro- and nanoparticles, including particles that do not have gas cores, has been investigated by a number of research groups. Although the acoustic response and release mechanisms can be different in the absence of a gas core, there are similarities in the targeting aspects, and those approaches that may be most applicable for microbubbles are also briefly mentioned here.

Some targeting approaches have primarily made use of charge for attachment of microbubbles to particular locations in the vasculature. For example, lipid-encapsulated microbubbles with a net negative charge can be retained within capillaries via complement-mediated attachment to endothelium [142]. Lipid-coated microbubbles have been shown to selectively accumulate in rat brain gliomas [110], and to increase the echogenicity of rat liver tumors [109]. Lipid coated microbubbles have also been found to be internalized by glioblastoma and gliosarcoma tumor cells *in vivo* and *in vitro*, with no evidence of them in the surrounding normal brain tissue in *in vivo* experiments [143].

Other targeting approaches have used specific microbubble shell materials, or conjugated monoclonal antibodies or other ligands to these shells, that recognize antigens expressed in regions of disease as a means to target delivery to the diseased tissue. The adhesion mechanisms in this type of targeted delivery are similar to the adhesion mechanisms involved in leukocyte adhesion, a process comprised of leukocyte rolling and attachment dynamics [144-154]. Similar targeting strategies are used in related micro- and nanoparticle drug delivery approaches [155,156]. A biotinylated, lipid-coated, perfluorocarbon contrast agent was demonstrated to target thrombi *in vivo* [157]. In another study, antibody-conjugated liposomes were shown to attach to fibrin on slides and to fibrous plaques of the arterial segments, whereas unconjugated liposomes did not [158]. A subsequent *in vivo* study showed that liposomes conjugated to antifibrinogen or anti-intercellular adhesion molecule (ICAM)-1 target atherosclerotic plaques and thrombi [159]. Another investigation showed that conjugating monoclonal antibodies against murine P-selectin to the lipid shell of microbubbles allowed them to target them to P-selectin [160]. Other targeting work included the development of an angiogenesis-targeted microbubble ultrasound contrast agent [161], targeted microbubble adhesion to atherosclerotic plaques [162], and perfluorobutane-filled microbubbles with anti-inflammatory marker ICAM-1 monoclonal antibodies conjugated to the lipid shell [163]. In related work, Weller *et al.* used targeted microbubbles to detect rejecting rat cardiac transplant myocardium [164]. A subsequent study demonstrated that microbubbles targeted to tumor vasculature via arginine–arginine–leucine preferentially adhered to tumor vasculature compared with normal vasculature [165]. Poly (lactic acid), (PLA), microcapsules conjugated with the Arg–Gly–Asp (RGD) peptide sequence were shown to adhere specifically to a breast cancer cell line MDA-MB-231 in static experiments [133] – a technique that could potentially be useful in drug delivery. Other work demonstrated the potential for microbubble-enhanced ultrasound to deliver an antisense oligodeoxynucleotide targeting the human androgen receptor into prostate tumors [166]. A number of investigations have examined the use of microbubbles for delivery of protein [167] and genetic material [168-171].

3.2 Approaches to enhance adhesion

The targeting strategies described above require that the functionalized microbubble become close enough to the vessel wall for binding to occur. This is similar to the process of leukocyte adhesion and can involve rolling prior to binding. Microbubbles behave similarly to red blood cells, and tend to be transported into the faster moving blood near the center of vessels rather than the slower moving regions near the vessel wall [172]. This poses a challenge to targeted adhesion, particularly in larger vessels. In the microcirculation, this behavior is also an obstacle to adhesion, but may be counteracted by hemodynamic effects [173]. There are several designs for the attachment of antibodies and ligands to the microbubble surface, some of which are intended to enhance adhesion by addressing the radial variation in velocity within the blood vessels and adhesion dynamics [117]. One design is to attach the ligand directly to the shell, either by conjugation of the ligand and shell molecules in a separate procedure prior to forming the microbubble [174] or by conjugation of the ligand with the shell of preformed molecules [160,175]. Attachment of ligands to preformed microbubbles may be covalent [175] or noncovalent [160]. Another design is to use spacer arms between the shell and ligand [73,176,177], as shown in **Figure 1**. This can enhance adhesion by increasing the number of ligands that can be attached to a microbubble of a particular size, increasing the likelihood of retention by the target after the initial collision. Flexible spacer arms, such as PEG, allow the ligand to interact with more of the target surface and to extend past the PEG brush that is sometimes included on the shell surface. These features result in a microbubble targeting system that increases the chance of adhesion compared with attaching ligands directly to the shell [117,178]. Attachment can be enhanced by varying polymer chain length and density [179,180]. As noted in Section 2, the addition of shell components can result a rich variety of phenomena when the microbubbles are acoustically driven and when they deflate due to gas loss. The specific behavior depends on the particular components of the shell and their surface activity. An investigation of microbubble adhesion and retention under shear flow demonstrated that accumulation and retention of targeted ultrasound contrast agents is possible under physiologic flow conditions, and noted that both are strongly influenced by shear stress and surface density of the target receptor [181]. A number of studies have examined targeted adhesion under high shear flow [182,183].

Another approach to enhance microbubble adhesion is to use acoustic radiation forces to direct microbubbles towards the vessel walls [184,185]. Microbubble [186] and liposome [138] adhesion under acoustic pressure, and microbubble adhesion to cultured endothelial cells [186] have been investigated. Rychak *et al.* examined the flow and acoustic conditions under which acoustic radiation force enhances adhesion, and provided evidence that acoustic radiation forces increases targeted microbubble adhesion, using an *in vitro* model [187]. Ultrasound radiation force was shown to enable targeted deposition of model drug carriers loaded on microbubbles [188]. Another study demonstrated that ultrasound radiation force modulates ligand availability on targeted contrast agents [189]. Dayton *et al.* used theory and experiments to demonstrate the displacement of perfluorocarbon nanoparticles in the direction of ultrasound propagation, and the feasibility of ultrasound enhanced particle internalization and therapeutic delivery [190]. Another approaches at improving adhesion in targeted delivery include making the microbubbles deformable to increase microbubble–endothelium adhesion contact area and stabilize adhesion [191].

4. Drug release dynamics

4.1 Acoustic driving of bubbles

As noted above, much of the initial interest in developing encapsulated microbubbles was motivated by their potential as ultrasound contrast agents and the fact that they can be designed to produce a unique signature within an acoustic field, and detection of this signature is the basis of contrast-enhanced ultrasound [1,4,5,132]. Microbubbles resonate with a natural frequency. The acoustic signature of a microbubble depends on the size, compressibility and density of the gas bubble, the viscosity and density of the surrounding liquid, the ultrasound frequency and power, and the presence of an encapsulating shell [94,192-195]. These acoustically induced bubble oscillations represent one form of acoustic driving of microbubbles, a form that is especially important for diagnostics.

Higher power ultrasound driving of microbubbles results in more extreme oscillation of the bubble radius. This is relevant to drug delivery via microbubble carriers because these large oscillations can lead to high vessel wall stresses and strong enough driving can cause microbubble collapse, thereby destroying the microbubble. Both of these have important implications for drug delivery. The ability to destroy microbubbles via ultrasound further enhances the site-specific delivery of drugs, and potentially improves drug efficacy while minimizing systemic adverse effects. Microbubble destruction releases the cargo in attachment and incorporation carrier designs (by fracturing the shell), by eliminating the bubble with the containment approach, and can enhance delivery in all four carrier approaches by enhancing vessel permeability [69,103,116,130-139,196-200]. A number of theoretical and experimental studies have examined microbubble destruction [201-208]. These studies have shown that bubble collapse can lead to the formation of jets that can impact the nearby vessel walls, potentially inducing bioeffects and changes in permeability. Experimental and theoretical investigations of microbubble destruction mechanisms for microbubbles demonstrated that fragmentation can lead to the rapid destruction of microbubbles on a time scale of microseconds [131]. Another study showed that destruction mechanism varies with initial radius,

for 0.5 – 12.0 μm diameter microbubbles with an outer lipid coating, an oil layer, and a perfluorobutane gas core [135]. Microbubbles smaller than resonance size were found to undergo symmetric collapse, but microbubbles between resonance size and twice resonance size exhibited asymmetrical oscillations. The destruction mode for microbubbles more than twice the resonance size is bubble pinch-off, with one fragment containing most of the original bubble volume. Christiansen *et al.* investigated the mechanisms of gene transfection by ultrasound destruction of plasmid-bearing microbubbles [209]. Microbubble destruction has also been shown to depend on the encapsulating shell constituents [210].

Microbubbles undergoing large oscillations while confined in small-diameter vessels, as in the microcirculation, can lead to high vessel wall stresses or vessel wall rupture, both of which affect the permeability of the vessels. Experiments with perfluorocarbon microbubbles demonstrated that microbubbles with bioactive albumin on their surface that can bind synthetic antisense oligonucleotides and then release them in the presence of diagnostic ultrasound [211]. An *in vitro* study of the acoustic driving of microbubbles for drug delivery showed that a train of ultrasound pulses can alter the structure of an albumin-shelled bubble, initiate various mechanisms of bubble destruction or produce aggregation [132]. Related studies also examined acoustic driving of microbubbles [97,101]. High-speed imaging experiments demonstrated that polymer-shelled microbubbles and lipid-shelled microbubbles exhibit different responses to acoustic pulses [100]. Microbubbles encapsulated in polymer shells did not oscillate significantly. Although a gas bubble was ejected through a shell defect, the shell appeared to remain mostly intact.

A computational study of the expansion of microbubbles resulting from acoustic droplet vaporization in essentially rigid microvessels demonstrated that smaller microbubble diameters, relative to the vessel radius, have less potential to damage or rupture vessel walls [212]. **Figure 2** shows pressure and shear stress along the vessel wall at various times during the growth phase (collapse is not shown), and the corresponding bubble shapes at the same times. The bubble diameter is initially half the vessel diameter, and only the right half of the domain is shown because it was considered to be symmetric. A similar computational investigation with a flexible vessel wall model by the same authors demonstrated that wall flexibility significantly reduces the wall stress and can substantially modify the flow field induced by the expanding bubble [213]. **Figure 3** shows the bubble shape at various times and the corresponding streamlines within the surrounding blood. The resulting flow field for a flexible vessel model is significantly different from that for a rigid vessel model. In-flow at the tube ends and out-flow near the bubble surface occur due to the combined effects of bubble and tube deformation. For sufficiently flexible walls, the expanding bubble pushes the vessel wall out fast enough that inflow towards the bubble occurs at the ends of the vessel. A subsequent investigation of ultrasound-induced microbubble oscillations also predicted that increasing vessel stiffness increases the circumferential stress in vessels and that decreasing the vessel size or the centre frequency increases the circumferential stress [214]. A related study investigated microbubble-induced bioeffects in shockwave lithotripsy [215].

4.2 Vessel permeability and dependence on acoustic driving

The acoustic driving of microbubbles has a significant impact on vessel wall stress and permeability, which in turn affect drug uptake. Price *et al.* [137] demonstrated the ability of ultrasound destruction of microbubbles in microvessels to deliver fluorescent red blood cells and polymer microspheres (205 and 503 nm in diameter) to the interstitium of skeletal muscle in an exteriorized rat spinotrapezius model, as shown in **Figure 4**. This study suggested the potential of acoustic destruction of microbubbles for delivery of particles or drug across the endothelium of the microcirculation of the target tissue. A related study examined the effects of microbubble destruction on surrounding tissue and demonstrated that microbubbles can be destroyed by ultrasound, resulting in a bioeffect that could be used for local drug delivery angiogenesis, and vascular remodeling, or for tumor destruction [139]. **Figure 5** shows the extravasation of red blood cells that resulted from microbubble destruction. These initial studies suggest the potential of acoustic driving of microbubbles to increase vessel permeability and enhance uptake of drugs by surrounding tissue. Subsequent studies have considered how to optimize parameters for specific delivery applications and cargo [200,209,216-219].

4.3 Microbubbles and ultrasound for localized opening of the blood–brain barrier

Related to the vessel permeability issues discussed in Section 4.2 is the specific application of microbubbles and ultrasound to the blood–brain barrier (BBB). This specialized system of capillary endothelial cells allows required nutrients to pass through while protecting the brain from harmful substances in the blood, and is a significant obstacle to drug delivery to the brain [220]. A number of studies have examined the potential for microbubble carriers to enable transport through the BBB. This work is described in detail elsewhere [221], and is briefly discussed here with an emphasis on its microbubble aspects.

Motivated by decompression sickness, Hills and James demonstrated that microbubbles impair the BBB integrity to protein [222]. An investigation of high-intensity pulsed ultrasound effects on the rabbit brain showed that histologic response depended on acoustic parameters, such as pulse duration, the number of pulses and repetition frequency, and that BBB breakage could be induced [223]. The same group later demonstrated that the BBB can be consistently opened with focused ultrasound exposures in the presence of a microbubble contrast agent [224]. A related study in a rabbit

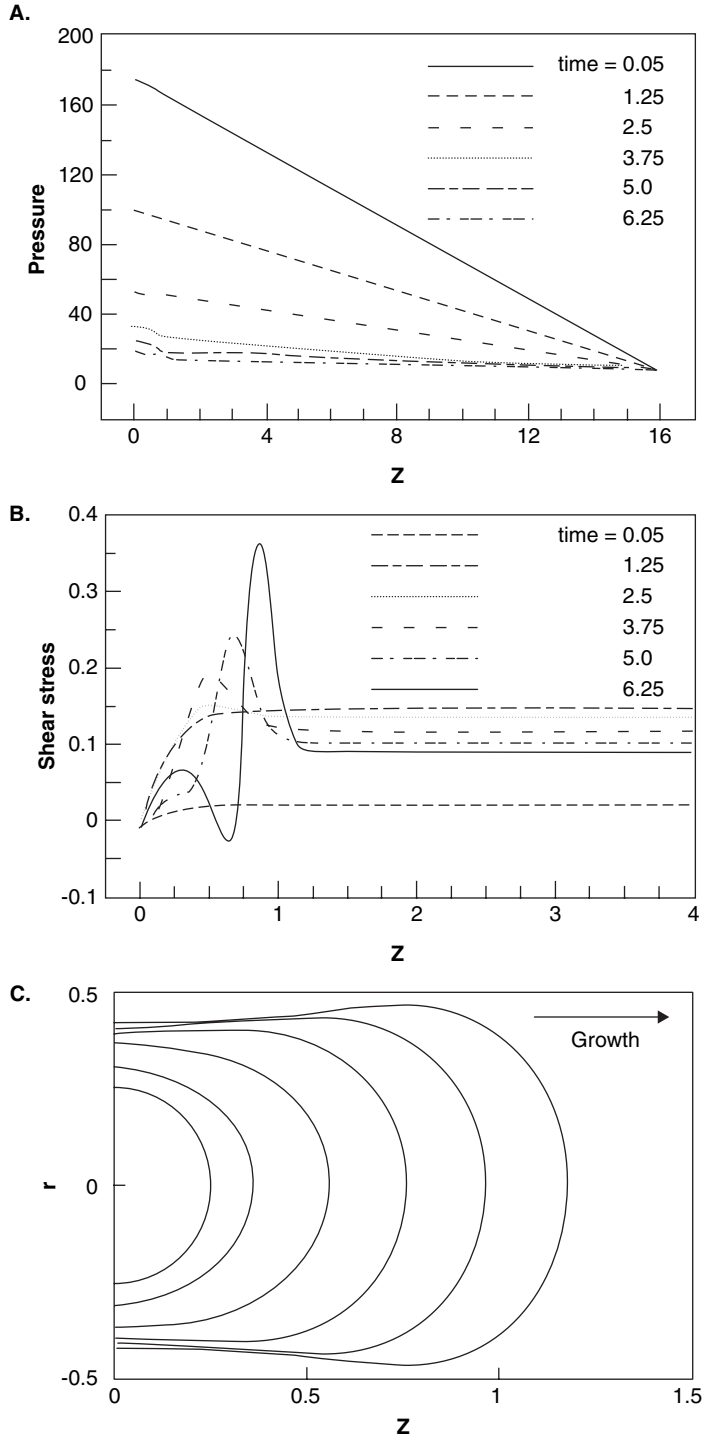

Figure 2. A. Pressure; and B. shear stress along the top wall of the tube at various times for the following parameter values: Reynolds number = 427.59, Weber number = 6.93, Strouhal number = 10.47, initial bubble pressure = 20 bar, and initial bubble diameter = 1/2 of the vessel diameter. The horizontal axis indicates axial position, z. Only the significant portion of the tube, $z \leq 4$, for shear stress is shown. The dimensional stress is 11,338.8 N/m^2 per dimensionless unit. **C**. Bubble shapes at times presented in **A**. and **B**.

Reproduced from YE T, BULL JL: Direct numerical simulations of micro-bubble expansion in gas embolotherapy. *J. Biomech. Eng.* (2004) **126**:745-759 with permission from ASME publications.

r: Radial position; z: Longitudinal position.

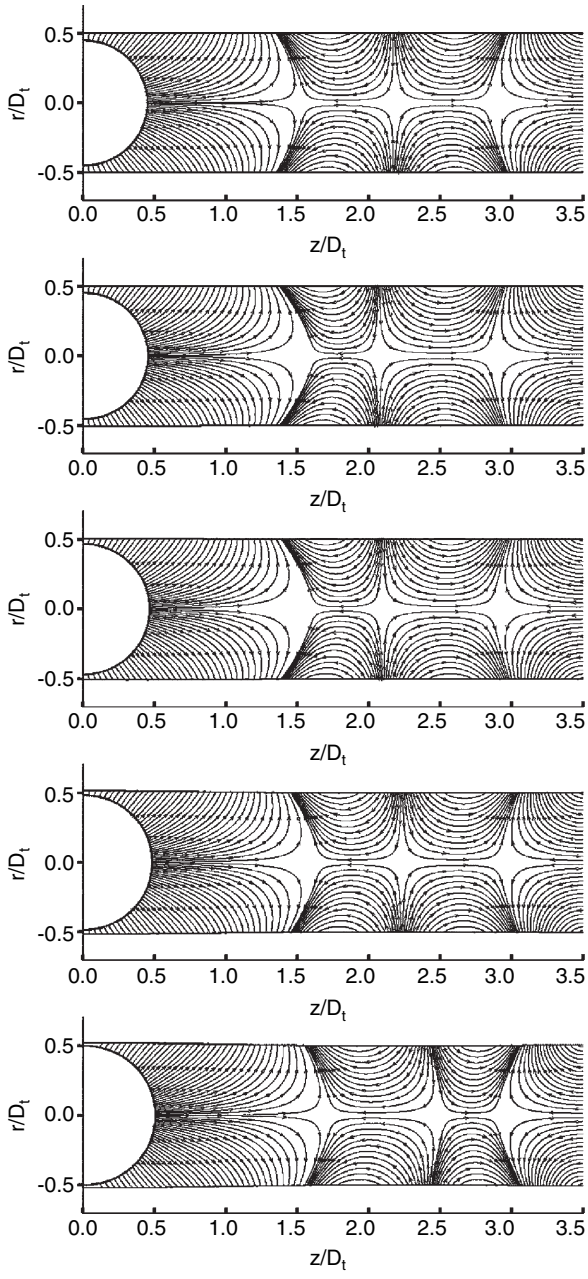

Figure 3. Bubble and wall shapes, and streamlines at dimensionless times t = 0.004, 0.4, 0.8, 1.2, and 1.6 for, for the same parameter values as in Figure 2 and dimensionless wall stiffness = $\Omega s = 5 \times 10^{-9}$, and dimensionless wall tension = $\Omega_t = 0.05$. Only half of the physical domain, $0 \leq z \leq 3.5$, is shown because of symmetry.

Reproduced from YE T, BULL JL: Microbubble expansion in a flexible tube. *J. Biomech. Eng.* (2006) **128**:554-563, with permission from ASME publications. D_t: Tube diameter; r: Radial position, z: Longitudinal position.

model showed that the ultrasound exposure levels typically used for blood flow measurements in the brain are below the threshold of BBB opening or brain tissue damage and noted that brain damage can be induced at increased exposure levels [225]. A separate investigation of alteration of the BBB from ultrasonic contrast agent destruction by diagnostic transcranial color-coded sonography suggested the safety of ultrasonic destruction of Levovist® (Schering AG) and Optison™ (GE Healthcare) microbubbles by diagnostic transcranial color-coded sonography [226]. However, the authors noted that more subtle local effects may have been missed by gadolinium-enhanced magnetic resonance imaging and suggested that studies on microbubble-based drug delivery strategies should consider ultrasonic contrast agent microbubble characteristics and concentration as well as ultrasound transmission power levels.

A later study suggested several mechanisms responsible for this transient opening of the BBB by ultrasound and microbubbles, including transcytosis; endothelial cell cytoplasmic openings-fenestration and channel formation; opening of a part of tight junctions; and free passage through the injured endothelium (with the higher power sonications) [227]. The ability of MRI-derived temperature information to better predict damage, compared with the ultrasound parameters, in this application was noted by McDannold *et al.* [228]. Subsequent studies in the rabbit model demonstrated i) completely noninvasive focal disruption of the BBB is possible [229]; ii) safety of the method for targeted drug delivery compared with presently available invasive methods [230]; iii) MRI-derived temperature measurements appeared to correlate with focused ultrasound-induced lesions in the brain when microbubbles were present, despite the temperature appearing to be below the threshold for thermal damage; and iv) BBB disruption can occur without indicators for inertial cavitation, suggesting that if inertial cavitation is not responsible for the disruption that other ultrasound–microbubble interactions likely are [231]. A related numerical simulation indicated the feasibility of transcranial ultrasound focusing with a non-moving phased array and without skull-specific aberration correction [232].

Further investigation in the rabbit model revealed that vesicle transport of tracer molecules was higher in brain arterioles than in capillaries and venules following ultrasound-induced opening of the BBB [233], and demonstrated the ability to provide temporary disruption of the BBB at targeted locations [234]. The ability to deliver antibodies across the BBB with this approach was also reported [235,236]. Raymond *et al.* used multiphoton microscopy to further investigate the permeabilization mechanism and immediate effects of ultrasound/microbubbles on the BBB [74]. Their results corroborated previous studies' suggestions of increased endothelial transcytosis and breached tight junctions, and also demonstrated vasoconstriction. McDannold *et al.* demonstrated the ability to produce temporary BBB disruption with the microbubble contrast agent Definity, rather than the Optison that the group had previously used [237]. They noted that under the conditions of their experiments, Optison produced a larger effect at the same acoustic pressure.

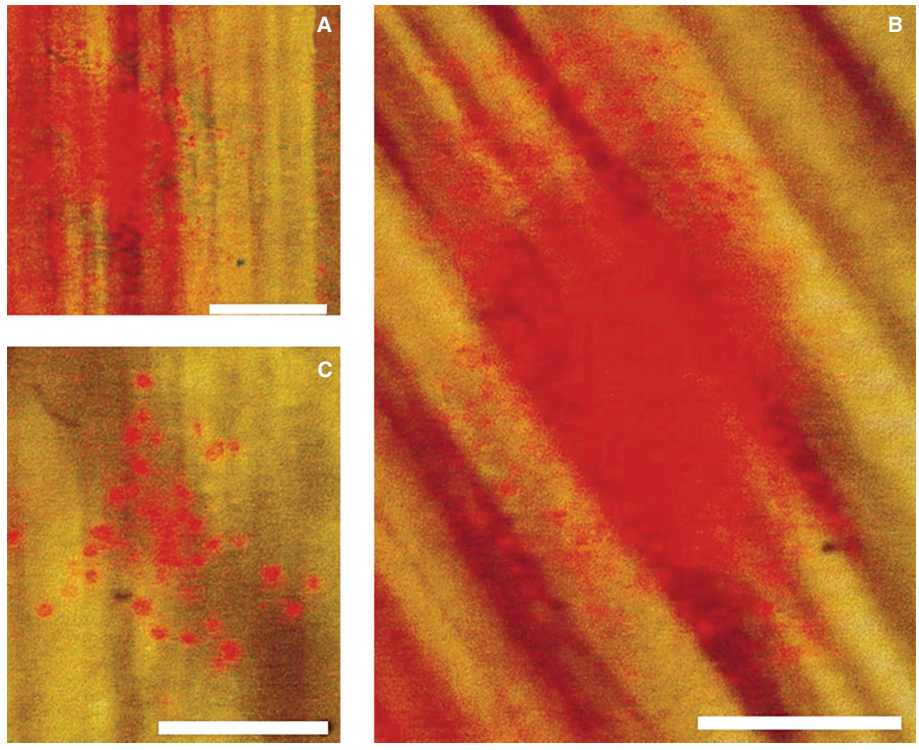

Figure 4. Combined transilluminated and epifluorescent images of red fluorescent 205-nm-diameter polymer microspheres (A), red fluorescent 503-nm-diameter polymer microspheres (B), and $DiIC_{18}$(3)-labeled red blood cells (C) that have been delivered to the interstitium of rat spinotrapezius muscle through microvessel ruptures created by application of a single frame of ultrasound.

Bars indicate 100 µm.

Reproduced from PRICE RJ, SKYBA DM, KAUL S, SKALAK TC: Delivery of colloidal particles and red blood cells to tissue through microvessel ruptures created by targeted microbubble destruction with ultrasound. *Circulation* (1998) **98**:1264-1267, with permission.

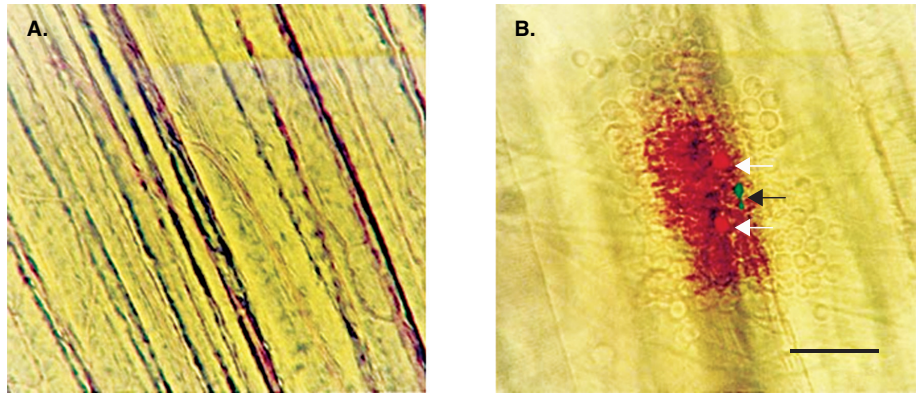

Figure 5. Intravital images of microvessels in rat spinotrapezius muscle. A. Normal muscle and intact capillaries under transillumination (×20 objective) after injection of microbubbles but before insonification with ultrasound. **B.** Composite image created from transilluminated and epi-illuminated images after ultrasound exposure in presence of microbubbles. Ruptured capillary with extravasation of red blood cells is shown. White arrows indicate propidium iodide-labeled nonviable cells; black arrow indicates fragments of destroyed microbubble. Scale bar = 20 µm.

Reproduced from SKYBA DM, PRICE RJ, LINKA AZ *et al.*: Direct *in vivo* visualization of intravascular destruction of microbubbles by ultrasound and its local effects on tissue. *Circulation* (1998) **98**:290-293, with permission.

In a separate study, Choi *et al.* demonstrated the feasibility of locally opening the BBB in mice using focused ultrasound through intact skull and skin, and noted the significance of this as a step towards localized drug delivery to the brain [238]. Coussios *et al.* presented models of how different types of cavitation activity, in the context of high-intensity focused ultrasound, can serve to accelerate tissue heating, and noted that their results suggest that the absorption of broadband acoustic emissions generated byinertial cavitation may be responsible for the bulk of the enhanced heating effect [239].

5. Microbubble clearance

Localized drug delivery is usually preferred to systemic delivery when drugs have either high toxicity or high cost. Microbubbles have been shown to be cleared from the blood by the liver or spleen [240-243]. Although hepatic clearance of perfluorobutane microbubbles by Kupffer cells has been shown to not reduce the ability of liver to phagocytose or degrade albumin microspheres [242], the impact of clearance of drug along with microbubbles has not been thoroughly investigated. The effects of the specific drug within the microbubble carrier on the liver will need to be examined for each drug, as effects will be drug dependent. If delivery can be confined to the tumor or other target region by a relatively high binding rate, the time the carriers spend in circulation will be reduced and, consequently, there will be less opportunity for uptake by the liver occurs before the microbubble carriers reach their target. Ideally, the drug-microbubble carrier would be non-toxic unless acoustically activated. For example, plasmid DNA in a microbubble carrier has been shown to have no detectable transfection in any tissues in the absence of ultrasound activation [209]. Even in less than ideal scenarios, microbubble carriers for localized delivery are anticipated to be far more efficient that systemic chemotherapy because of their potential for greatly reducing the overall dose size and exposure of non-tumor tissues to chemotherapeutics.

6. Conclusions

There has been much recent progress in the development of microbubble carriers for drug delivery and in the corresponding targeting approaches. Effective localized delivery of drugs and genetic material via microbubbles would have a significant clinical impact by reducing toxicity side effects and potential cost reduction. Work in this area has demonstrated the feasibility of many targeting approaches for many targets, and has provided a basis for further optimization of microbubble carrier designs.

7. Expert opinion

Progress in the development of microbubble carriers for drug delivery and in novel targeting approaches, along with the availability of ultrasound equipment in the clinic, creates a foundation for translation of many of these developmental approaches to localized drug delivery. Despite this success, there are still many questions and limitations that must be addressed before these approaches can be considered for use in patients. A better understanding of bioeffects and vessel permeability induced by acoustically driven microbubbles and the related bubble dynamics will be essential to developing sophisticated strategies for the delivery of cargo from microbubbles. A more complete understanding of the underlying fundamental biofluid mechanics is needed to address those questions. As noted in a number of the studies described here, many of these questions related to drug delivery and induced permeability changes are difficult to address *in vivo*, and the mechanisms involved are complicated and numerous. Several of these investigations have noted the likely involvement of interfacial dynamics and gas transport in the resulting microbubble behavior and physiologic response. Biofluid mechanics approaches will also provide important information regarding the effects of microbubble deformation, orientation and rotation on stability, production of bioeffects and targeted drug delivery. Most theoretical and computational analyses of acoustically driven microbubbles have either ignored the presence of drug cargo or considered it in an idealized manner. As the incorporation of the drug into the microbubble carriers becomes more sophisticated, more complete and realistic characterizations will be needed to optimize carrier designs and performance. Encapsulation and adhesion approaches by themselves also present some challenges. For example, shell materials would ideally be stable enough that the microbubble carriers would not rupture or release their cargo until activated, but would have properties that would provide sufficient acoustic response to induce changes in vessel permeability when activated. Depending on the designs used, the incorporation of drugs and ligands for attachment into microbubbles could conceivably enhance or reduce microbubble stability. Recent advances in high-speed imaging and in computational resources are expected to enable the necessary biofluid mechanics advances, through experimental and computational investigations of microbubble dynamics and microbubble interactions with vessels and cellular components of blood.

Further transport of drugs once they permeate the endothelium is needed to treat solid tumors, and this may be partially addressed by microbubble-induced bioeffects and by further development of drug vehicles carried by the microbubbles. Optimization of targeting approaches, binding efficiency, shell and gas components will be needed to tailor microbubble carriers to particular applications. Similarly, clearance of drug-loaded microbubble carriers and their effects will need to be investigated for each design. These microbubble drug carriers will have to be tested in large animal models, and advances in ultrasound technology may

be required to allow selective activation of microbubble carriers in target tissues. More detailed studies of benefits and risks in animal models of human diseases, including the related response of pathological tissues, will be needed to determine which drug and disease scenarios may be viable for treatment by this approach. Progress in these areas will be needed before clinical trials can begin. Success in these areas could lead to a means for localized delivery that would potentially have significant clinical impact.

Acknowledgements

This work was supported by NIH Grant Number EB003541 and NSF Grant Number BES-0301278.

Bibliography

Papers of special notes have been highlighted as either of interest (•) or of considerable interest (••) to readers.

1. BULL JL: Cardiovascular bubble dynamics. *Crit. Rev. Biomed. Eng.* (2005) **33**(4):299-346.
• **Reviews a variety of microbubble topics.**
2. KLIBANOV AL: Ultrasound contrast agents: development of the field and current status. *Top. Curr. Chem.* (2002) **222**:73-106.
• **Very thorough review of contrast agents.**
3. CHAPPELL JC, PRICE RJ: Targeted therapeutic applications of acoustically active microspheres in the microcirculation. *Microcirculation* (2006) **13**(1):57-70.
• **Contains a table summary of *in vivo* delivery experiments.**
4. LINDNER JR: Microbubbles in medical imaging: current applications and future directions. *Nat. Rev. Drug Discov.* (2004) **3**(6):527-532.
5. KLIBANOV AL: Microbubble contrast agents – targeted ultrasound imaging and ultrasound-assisted drug-delivery applications. *Invest. Radiol.* (2006) **41**(3):354-362.
6. KU DN: Blood flow in arteries. *Annu. Rev. Fluid Mech.* (1997) **29**:399-434.
7. PEDLEY TJ: *The Fluid Mechanics of Large Blood Vessels* (Ed.), Cambridge University Press, Cambridge (1980):446.
8. FUNG YC: *Biomechanics: Motion, Flow, Stress, and Growth* (Ed.), Springer-Verlag, New York (1990):569.
9. FUNG YC: *Biomechanics: Circulation* (Ed.), Springer, New York (1997):571.
10. *Modeling and Simulation of Capsules and Biological Cells*. Pozrikidis C (Ed.), Chapman & Hall/CRC, Boca Raton, FL (2003).
11. BLYTH MG, POZRIKIDIS C: Solution space of axisymmetric capsules enclosed by elastic membranes. *Eur. J. Mech. A Solids* (2004) **23**(5):877-892.
12. POZRIKIDIS C: Numerical simulation of the flow-induced deformation of red blood cells. *Ann. Biomed. Eng.* (2003) **31**(10):1194-1205.
13. HALPERN D, SECOMB TW: The squeezing of red blood-cells through capillaries with near-minimal diameters. *J. Fluid Mech.* (1989) **203**:381-400.
14. HALPERN D, SECOMB TW: The squeezing of red-blood-cells through parallel-sided channels with near-minimal widths. *J. Fluid Mech.* (1992) **244**:307-322.
15. SECOMB TW, HSU R, PRIES AR: Motion of red blood cells in a capillary with an endothelial surface layer: effect of flow velocity. *Am. J. Physiol. Heart Circ. Physiol.* (2001) **281**(2):H629-H636.
16. SECOMB TW, HSU R, PRIES AR: Blood flow and red blood cell deformation in nonuniform capillaries: effects of the endothelial surface layer. *Microcirculation* (2002) **9**(3):189-196.
17. MARUVADA S, HYNYNEN K: Optical monitoring of ultrasound-induced bioeffects in glass catfish. *Ultrasound Med. Biol.* (2004) **30**(1):67-74.
18. RIESS JG: Fluorocarbon-based injectable gaseous microbubbles for diagnosis and therapy. *Curr. Opin. Coll. Interf. Sci.* (2003) **8**(3):259-266.
19. BREYIANNIS G, POZRIKIDIS C: Simple shear flow of suspensions of elastic capsules. *Theor. Comput. Fluid Dyn.* (2000) **13**(5):327-347.
20. EGGLETON CD, POPEL AS: Large deformation of red blood cell ghosts in a simple shear flow. *Phys. Fluids* (1998) **10**(8):1834-1845.
21. RAMANUJAN S, POZRIKIDIS C: Deformation of liquid capsules enclosed by elastic membranes in simple shear flow: large deformations and the effect of fluid viscosities. *J. Fluid Mech.* (1998) **361**:117-143.
22. LOEWENBERG M, HINCH EJ: Numerical simulation of a concentrated emulsion in shear flow. *J. Fluid Mech.* (1996) **321**:395-419.
23. LI XF, CHARLES R, POZRIKIDIS C: Simple shear flow of suspensions of liquid drops. *J. Fluid Mech.* (1996) **320**:395-416.
24. ZHOU H, POZRIKIDIS C: Deformation of liquid capsules with incompressible interfaces in simple shear-flow. *J. Fluid Mech.* (1995) **283**:175-200.
25. KENNEDY MR, POZRIKIDIS C, SKALAK R: Motion and deformation of liquid-drops, and the rheology of dilute emulsions in simple shear-flow. *Comput. Fluids* (1994) **23**(2):251-278.
26. SECOMB TW, STYP-REKOWSKA B, PRIES AR: Two-dimensional simulation of red blood cell deformation and lateral migration in microvessels. *Ann. Biomed. Engl.* (2007) **35**(5):755-765.
27. KELLER SR, SKALAK R: Motion of a tank-treading ellipsoidal particle in a shear-flow. *J. Fluid Mech.* (1982) **120**:27-47.
28. LIU SQ: Biomechanical basis of vascular tissue engineering. *Crit. Rev. Biomed. Eng.* (1999) **27**(1-2):75-148.
29. TAYLOR CA, DRANEY MT: Experimental and computational methods in cardiovascular fluid mechanics. *Annu. Rev. Fluid Mech.* (2004) **36**:197-231.
30. WOOTTON DM, KU DN: Fluid mechanics of vascular systems, diseases, and thrombosis. *Annu. Rev. Biomed. Eng.* (1999) **1**:299-329.
31. BERGER SA, JOU LD: Flows in stenotic vessels. *Annu. Rev. Fluid Mech.* (2000) **32**:347-382.
32. SEYMOUR RS, HARGENS AR, PEDLEY TJ: The heart works against gravity. *Am. J. Physiol.* (1993) **265**(4):R715-R720.
33. POPEL AS: Theory of oxygen-transport to tissue. *Crit. Rev. Biomed. Eng.* (1989) **17**(3):257-321.
34. SKALAK R, OZKAYA N, SKALAK TC: Biofluid mechanics. *Annu. Rev. Fluid Mech.* (1989) **21**:167-204.

35. BERGER SA, TALBOT L, YAO LS: Flow in curved pipes. *Annu. Rev Fluid Mech.* (1983) **15**:461-512.
36. GOLDSMITH HL, SKALAK R: Hemodynamics. *Annu. Rev. Fluid Mech.* (1975) 7:213-247.
37. FUNG YC, ZWEIFACH BW: Microcirculation – mechanics of blood flow in capillaries. *Annu. Rev. Fluid Mech.* (1971) **3**:189-210.
38. JONES RT: Blood flow. *Annu. Rev. Fluid Mech.* (1969) **1**:223-244.
39. MARANGONI C: On the expansion of a drop of liquid floating on the surface of another liquid. *Tipographia dei fratelli Fusi* (1965).
40. THOMSON J: On certain curious motions observable at the surfaces of wine and other alcholic liquors. *Phil. Mag.* (1855) **10**:330.
41. GUGLIOTTI M: Tears of wine. *J. Chem. Educ.* (2004) **81**(1):67-68.
42. YEO LY, CRASTER RV, MATAR OK: Marangoni instability of a thin liquid film resting on a locally heated horizontal wall. *Phys. Rev. E* (2003) **67**(5).
43. HOSOI AE, BUSH JWM: Evaporative instabilities in climbing films. *J. Fluid Mech.* (2001) **442**:217-239.
44. SILVERSTEIN TP: Why do alcoholic beverages have "legs"? *J. Chem. Educ.* (1998) **75**(6):723-724.
45. WALKER J: What causes the tears that form on the inside of a glass of wine. *Scientific American* (1983) **248**(5):162.
46. SCRIVEN LE, STERNLING CV: Marangoni effects. *Nature* (1960) **187**(4733):186-188.
47. EDWARDS DA, BRENNER H, WASAN DT: *Interfacial Transport Processes and Rheology* (Ed.), Butterworth-Heinemann, Boston, MA (1991).
48. POZRIKIDIS C: *Introduction to Theoretical and Computational Fluid Dynamics* (Ed.), Oxford University Press, Oxford (1997).
49. POZRIKIDIS C: Interfacial dynamics for stokes flow. *J. Comp. Phys.* (2001) **169**:250-301.
50. SHYY W: *Computational Modeling for Fluid Flow and Interfacial Transport* (Ed.), Elsevier, New York (1994).
51. SLATTERY JC: *Interfacial Transport Phenomena* (Ed.), Springer-Verlag, New York (1990).
52. POZRIKIDIS C: *Boundary Integral and Singularity Methods for Linearized Viscous Flow* (Ed.), Cambridge University Press (1992):259.
53. BULL JL, GROTBERG JB: Surfactant spreading on thin viscous films: film thickness evolution and periodic wall stretch. *Exp. Fluids* (2003) **34**:1-15.
54. BULL JL, NELSON LK, WALSH JT *et al.*: Surfactant-spreading and surface-compression disturbance on a thin viscous film. *J. Biomech. Eng.* (1999) **121**(1):89-98.
55. BULL JL, TREDICI S, KOMORI E *et al.*: Distribution dynamics of perfluorocarbon delivery to the lungs: an intact rabbit model. *J. Appl. Physiol.* (2004) **96**(5):1633-1642.
56. GROTBERG JB: Pulmonary flow and transport phenomena. *Annu. Rev. Fluid. Mech.* (1994) **26**:529-571.
57. GROTBERG JB: Respiratory fluid mechanics and transport processes. *Annu. Rev. Biomed. Eng.* (2001) **3**:421-457.
58. HALPERN D, BULL JL, GROTBERG JB: The effect of airway wall motion on surfactant delivery. *J. Biomech. Eng.* (2004) **126**(4):410-419.
59. HALPERN D, GAVER DP: Boundary element analysis of the time-dependent motion of a semi-infinite bubble in a channel. *J. Comp. Phys.* (1994) **115**(2): 366-375.
60. KAY SS, BILEK AM, DEE KC, GAVER DP: Pressure gradient, not exposure duration, determines the extent of epithelial cell damage in a model of pulmonary airway reopening. *J. Appl. Physiol.* (2004) **97**(1):269-276.
61. GHADIALI SN, GAVER DP: The influence of non-equilibrium surfactant dynamics on the flow of a semi-infinite bubble in a rigid cylindrical capillary tube. *J. Fluid Mech.* (2003) **478**:165-196.
62. GAVER DP, GROTBERG JB: droplet spreading on a thin viscous film. *J. Fluid Mech.* (1992) **235**:399-414.
63. GAVER DP, GROTBERG JB: The dynamics of alocalized surfactant on a thin-film. *J. Fluid Mech.* (1990) **213**:127-148.
64. GHADIALI SN, BANKS J, SWARTS JD: Effect of surface tension and surfactant administration on Eustachian tube mechanics. *J. Appl. Physiol.* (2002) **93**(3):1007-1014.
65. BRAUN RJ, FITT AD: Modelling drainage of the precorneal tear film after a blink. *Ima. J. Math. Appl. Med. Biol.* (2003) **20**(1):1-28.
66. BERGER RE, CORRSIN S: Surface-tension gradient mechanism for driving precorneal tear film after a blink. *J. Biomech.* (1974) 7(3):225.
67. FURGESON DY, DREHER MR, CHILKOTI A: Structural optimization of a "smart" doxorubicin–polypeptide conjugate for thermally targeted delivery to solid tumors. *J. Control. Rel.* (2006) **110**(2):362-369.
68. GEWIRTZ DA: A critical evaluation of the mechanisms of action proposed for the antitumor effects of the anthracycline antibiotics adriamycin and daunorubicin. *Biochem. Pharmacol.* (1999) **57**(7):727-741.
69. TACHIBANA K, TACHIBANA S: The use of ultrasound for drug delivery. *Echocardiography* (2001) **18**(4):323-328.
70. LIU YY, MIYOSHI H, NAKAMURA M: Encapsulated ultrasound microbubbles: therapeutic application in drug/gene delivery. *J. Control. Rel.* (2006) **114**(1):89-99.
71. LIU Y, YANG H, SAKANISHI A: Ultrasound: mechanical gene transfer into plant cells by sonoporation. *Biotechnol. Adv.* (2006) **24**(1):1-16.
72. LIU Y, UNO H, TAKATSUKI H, HIRANO M, SAKANISHI A: Interrelation between HeLa-S3 cell transfection and hemolysis in red blood cell suspension using pulsed ultrasound of various duty cycles. *Eur. Biophys. J. Biophys. Lett.* (2005) **34**(2):163-169.
73. WU YQ, UNGER EC, MCCREERY TP *et al.*: Binding and lysing of blood clots using MRX-408. *Investig. Radiol.* (1998) **33**(12):880-885.
74. RAYMOND SB, SKOCH J, HYNYNEN K, BACSKAI BJ: Multiphoton imaging of ultrasound/optison mediated cerebrovascular effects *in vivo*. *J. Cereb. Blood Flow Metab.* (2007) **27**(2):393-403.
75. SMITH MD, ELION JL, MCCLURE RR *et al.*: Left heart opacification with peripheral venous injection of a new saccharide echo contrast agent in dogs. *J. Am. College Cardiol.* (1989) **13**(7):1622-1628.
76. SMITH MD, KWAN OL, REISER HJ, DEMARIA AN: Superior intensity and

reproducibility of shu-454, a new right heart contrast agent. *J. Am. College Cardiol.* (1984) **3**(4):992-998.

77. FEINSTEIN SB, CHEIRIF J, TENCATE FJ *et al.*: Safety and efficacy of a new transpulmonary ultrasound contrast agent – initial multicenter clinical-results. *J. Am. College Cardiol.* (1990) **16**(2):316-324.
78. SIMON RH, HO SY, DARRIGO J, WAKEFIELD A, HAMILTON SG: Lipid-coated ultrastable microbubbles as a contrast agent in neurosonography. *Investig. Radiol.* (1990) **25**(12):1300-1304.
79. SCHNEIDER M, BROILLET A, BUSSAT P *et al.*: Gray-scale liver enhancement in VX2 tumor-bearing rabbits using BR14, a new ultrasonographic contrast agent. *Investig. Radiol.* (1997) **32**(7):410-417.
80. MEZA M, GREENER Y, HUNT R *et al.*: Myocardial contrast echocardiography: reliable, safe, and efficacious myocardial perfusion assessment after intravenous injections of a new echocardiographic contrast agent. *Am. Heart J.* (1996) **132**(4):871-881.
81. FRITZ TA, UNGER EC, SUTHERLAND G, SAHN D: Phase I clinical trials of MRX-115 – a new ultrasound contrast agent. *Investig. Radiol.* (1997) **32**(12):735-740.
82. PORTER TR, XIE F, KRICSFELD A, KILZER K: Noninvasive identification of acute myocardial-ischemia and reperfusion with contrast ultrasound using intravenous perfluoropropane-exposed sonicated dextrose albumin. *J. Am. College Cardiol.* (1995) **26**(1):33-40.
83. FORSBERG F, BASUDE R, LIU JB *et al.*: Effect of filling gases on the backscatter from contrast microbubbles: theory and *in vivo* measurements. *Ultrasound Med. Biol.* (1999) **25**(8):1203-1211.
84. PELURA TJ: Clinical experience with AF0150 (Imagent US), a new ultrasound contrast agent. *Acad. Radiol.* (1998) **5**:S69-S71.
85. DARRIGO JS, SAIZJIMENEZ C, REIMER NS: Geochemical properties and biochemical-composition of the surfactant mixture surrounding natural microbubbles in aqueous-media. *J. Coll. Interf. Sci.* (1984) **100**(1):96-105.
86. DARRIGO JS: Surface-properties of microbubble surfactant monolayers at the air water interface. *J. Coll. Interf. Sci.* (1984) **100**(1):106-111.
87. DARRIGO JS: Biological surfactants stabilizing natural microbubbles in aqueous-media. *Adv. Coll. Interf. Sci.* (1983) **19**(4):253-307.
88. DARRIGO JS: Aromatic proteinaceous surfactants stabilize long-lived gas microbubbles from natural sources. *J. Chem. Phys.* (1981) **75**(2):962-968.
89. DARRIGO JS: Structural features of the non-ionic surfactants stabilizing long-lived bubble nuclei. *J. Chem. Phys.* (1980) **72**(9):5133-5138.
90. DARRIGO JS: Physical-properties of the non-ionic surfactants surrounding gas cavitation nuclei. *J. Chem. Phys.* (1979) **71**(4):1809-1813.
91. YOUNT DE, KUNKLE TD, DARRIGO JS *et al.*: Stabilization of gas cavitation nuclei by surface-active compounds. *Aviation Space Environ. Med.* (1977) **48**(3):185-191.
92. DARRIGO JS, IMAE T: Physical characteristics of ultrastable lipid-coated microbubbles. *J. Coll. Interf. Sci.* (1992) **149**(2):592-595.
93. DARRIGO JS, HO SY, WAKEFIELD AE *et al.*: Lipid-coated, uniform microbubbles for earlier ultrasonic-detection of brain-tumors. *Abstr. Papers Am. Chem. Soc.* (1990) **199**:82.
94. DEJONG N, HOFF L, SKOTLAND T, BOM N: Absorption and scatter of encapsulated gas filled microspheres – theoretical considerations and some measurements. *Ultrasonics* (1992) **30**(2):95-103.
95. WHEATLEY MA, SINGHAL S: Structural studies on stabilized microbubbles – development of a novel contrast agent for diagnostic ultrasound. *React. Polym.* (1995) **25**(2-3):157-166.
96. NARAYAN P, WHEATLEY MA: Preparation and characterization of hollow microcapsules for use as ultrasound contrast agents. *Polym. Eng. Sci.* (1999) **39**(11):2242-2255.
97. ALLEN JS, KRUSE DE, DAYTON PA, FERRARA KW: Effect of coupled oscillations on microbubble behavior. *J. Acoust. Soc. Am.* (2003) **114**(3):1678-1690.
98. ALLEN JS, KRUSE DE, FERRARA KW: Shell waves and acoustic scattering from ultrasound contrast agents. *IEEE Trans. Ultrason. Ferroelectr. Freq. Control.* (2001) **48**(2):409-418.
99. BASUDE R, WHEATLEY MA: Generation of ultraharmonics in surfactant based ultrasound contrast agents: use and advantages. *Ultrasonics* (2001) **39**(6):437-444.
100. BLOCH SH, WAN M, DAYTON PA, FERRARA KW: Optical observation of lipid- and polymer-shelled ultrasound microbubble contrast agents. *Appl. Phys. Lett.* (2004) **84**(4):631-633.
101. PATEL D, DAYTON P, GUT J, WISNER E, FERRARA KW: Optical and acoustical interrogation of submicron contrast agents. *IEEE Trans. Ultrason. Ferroelectr. Freq. Control.* (2002) **49**(12):1641-1651.
102. PATEL DN, BLOCH SH, DAYTON PA, FERRARA KW: Acoustic signatures of submicron contrast agents. *IEEE Trans. Ultrason. Ferroelectr. Freq. Control.* (2004) **51**(3):293-301.
103. TACHIBANA K, TACHIBANA S: Albumin microbubble echo-contrast material as an enhancer for ultrasound accelerated thrombolysis. *Circulation* (1995) **92**(5):1148-1150.
104. WANG WH, MOSER CC, WHEATLEY MA: Langmuir trough study of surfactant mixtures used in the production of a new ultrasound contrast agent consisting of stabilized microbubbles. *J. Phys. Chem.* (1996) **100**(32):13815-13821.
105. SINGHAL S, MOSER CC, WHEATLEY MA: Surfactant-stabilized microbubbles as ultrasound contrast agents – stability study of span-60 and tween-80 mixtures using a langmuir trough. *Langmuir* (1993) **9**(9):2426-2429.
106. FORSBERG F, WU YQ, MAKIN IRS, WANG WH, WHEATLEY MA: Quantitative acoustic characterization of a new surfactant-based ultrasound contrast agent. *Ultrasound Med. Biol.* (1997) **23**(8):1201-1208.
107. BASUDE R, DUCKWORTH JW, WHEATLEY MA: Influence of environmental conditions on a new surfactant-based contrast agent: ST68. *Ultrasound Med. Biol.* (2000) **26**(4):621-628.
108. SIMON RH, HO SY, LANGE SC, UPHOFF DF, DARRIGO JS: Applications of lipid-coated microbubble ultrasonic contrast to tumor-therapy.

Ultrasound Med. Biol. (1993) **19**(2):123-125.

109. DARRIGO JS, HO SY, SIMON RH: Detection of experimental rat-liver tumors by contrast-assisted ultrasonography. *Investig. Radiol.* (1993) **28**(3):218-222.
110. SIMON RH, HO SY, PERKINS CR, DARRIGO JS: Quantitative assessment of tumor enhancement by ultrastable lipid-coated microbubbles as a sonographic contrast agent. *Investig. Radiol.* (1992) **27**(1):29-34.
111. SINGHAL S, SCHROPE B, WHEATLEY M: Biomedical aspects of ultrasound contrast using polymeric microspheres. *Abstr. Papers Am. Chem. Soc.* (1992) **203**:46.
112. WHEATLEY M, SCHROPE B, SHEN P: Polymeric systems for diagnostic ultrasound contrast agents. *Abstr. Papers Am. Chem. Soc.* (1990) **200**:32.
113. SHEN P, WHEATLEY M: Polymer-coated microbubbles – a novel contrast agent for diagnostic ultrasound. *Abstr. Papers Am. Chem. Soc.* (1990) **199**:74.
114. EL-SHERIF DM, WHEATLEY MA: Development of a novel method for synthesis of a polymeric ultrasound contrast agent. *J. Biomed. Mater. Res. Part A* (2003) **66A**(2):347-355.
115. TOBIAS CA, DHOOT NO, WHEATLEY MA *et al.*: Grafting of encapsulated BDNF-producing fibroblasts into the injured spinal cord without immune suppression in adult rats. *J. Neurotrauma* (2001) **18**(3):287-301.
116. DHOOT NO, WHEATLEY MA: Microencapsulated liposomes in controlled drug delivery: strategies to modulate drug release and eliminate the burst effect. *J. Pharmaceut. Sci.* (2003) **92**(3):679-689.
117. KLIBANOV AL: Ligand-carrying gas-filled microbubbles: ultrasound contrast agents for targeted molecular imaging. *Bioconjugate Chem.* (2005) **16**(1):9-17.
118. CHIANG CW, LIN FC, FU M *et al.*: Importance of adequate gas-mixing in contrast echocardiography. *Chest* (1986) **89**(5):723-726.
119. HETTIARACHCHI K, TALU E, LONGO ML, DAYTON PA, LEE AP: On-chip generation of microbubbles as a practical technology for manufacturing contrast agents for ultrasonic imaging. *Lab. Chip* (2007) 7(4):463-468.
120. BOKOR D, CHAMBERS JB, REES PJ *et al.*: Clinical safety of SonoVue (TM), a new contrast agent for ultrasound imaging, in healthy volunteers and in patients with chronic obstructive pulmonary disease. *Investig. Radiol.* (2001) **36**(2):104-109.
121. KLIBANOV AL, GU H, WOJDYLA JK *et al.*: Attachment of ligands to gas-filled microbubbles via PEG spacer and lipid residues anchored at the interface. *Proceedings of 26th International Symposium on Controlled Release of Bioactive Materials.* Boston (1999).
122. HAUFF P, SEEMANN S, RESZKA R *et al.*: Evaluation of gas-filled microparticles and sonoporation as gene delivery system: feasibility study in rodent tumor models. *Radiology* (2005) **236**(2):572-578.
123. BORDEN MA, LONGO ML: Dissolution behavior of lipid monolayer-coated, air-filled microbubbles: effect of lipid hydrophobic chain length. *Langmuir* (2002) **18**(24):9225-9233.
124. BORDEN MA, PU G, RUNNER GJ, LONGO ML: Surface phase behavior and microstructure of lipid/PEG-emulsifier monolayer-coated microbubbles. *Coll. Surf. B Biointerf.* (2004) **35**(3-4):209-223.
125. PU G, BORDEN MA, LONGO ML: Collapse and shedding transitions in binary lipid monolayers coating microbubbles. *Langmuir* (2006) **22**(7):2993-2999.
126. BORDEN MA, MARTINEZ GV, RICKER J *et al.*: Lateral phase separation in lipid-coated microbubbles. *Langmuir* (2006) **22**(9):4291-4297.
127. KLIBANOV AL, FERRARA KW, HUGHES MS *et al.*: Direct video microscopic observation of the dynamic effects of medical ultrasound on ultrasound contrast microspheres. *Investig. Radiol.* (1998) **33**(12):863-870.
128. KLIBANOV AL, HUGHES MS, WOJDYLA JK, WIBLE JH, BRANDENBURGER GH: Destruction of contrast agent microbubbles in the ultrasound field: the fate of the microbubble shell and the importance of the bubble gas content. *Acad. Radiol.* (2002) **9**:S41-S45.
129. LANKFORD M, BEHM CZ, YEH J *et al.*: Effect of microbubble ligation to cells on ultrasound signal enhancement – implications for targeted imaging. *Investig. Radiol.* (2006) **41**(10):721-728.
130. ALLEN JS, MAY DJ, FERRARA KW: Dynamics of therapeutic ultrasound contrast agents. *Ultrasound Med. Biol.* (2002) **28**(6):805-816.
131. CHOMAS JE, DAYTON P, ALLEN J, MORGAN K, FERRARA KW: Mechanisms of contrast agent destruction. *IEEE Trans. Ultrason. Ferroelectr. Freq. Control.* (2001) **48**(1):232-248.
132. DAYTON PA, MORGAN KE, KLIBANOV AL, BRANDENBURGER GH, FERRARA KW: Optical and acoustical observations of the effects of ultrasound on contrast agents. *IEEE Trans. Ultrason. Ferroelectr. Freq. Control.* (1999) **46**(1):220-232.
133. LATHIA JD, LEODORE L, WHEATLEY MA: Polymeric contrast agent with targeting potential. *Ultrasonics* (2004) **42**(1-9):763-768.
134. LINDNER JR, KAUL S: Delivery of drugs with ultrasound. *Echocardiography* (2001) **18**(4):329-337.
135. MAY DJ, ALLEN JS, FERRARA KW: Dynamics and fragmentation of thick-shelled microbubbles. *IEEE Trans. Ultrason. Ferroelectr. Freq. Control.* (2002) **49**(10):1400-1410.
136. PARIKH SA, EDELMAN ER: Endothelial cell delivery for cardiovascular therapy. *Adv. Drug Deliv. Rev.* (2000) **42**(1-2):139-161.
137. PRICE RJ, SKYBA DM, KAUL S, SKALAK TC: Delivery of colloidal, particles and red blood cells to tissue through microvessel ruptures created by targeted microbubble destruction with ultrasound. *Circulation* (1998) **98**(13):1264-1267.
- **Demonstrated the ability to delivery cargo by microbubble destruction *in vivo*.**

138. SHORTENCARIER MJ, DAYTON PA, BLOCH SH *et al.*: A method for radiation-force localized drug delivery using gas-filled lipospheres. *IEEE Trans. Ultrason. Ferroelectr. Freq. Control.* (2004) **51**(7):822-831.
139. SKYBA DM, PRICE RJ, LINKA AZ, SKALAK TC, KAUL S: Direct *in vivo* visualization of intravascular destruction of microbubbles by ultrasound and its local effects on tissue. *Circulation* (1998) **98**(4):290-293.
- **Demonstrated bioeffects from microbubble destruction *in vivo*.**

140. HU YT, QIN SP, JIANG Q: Characteristics of acoustic scattering front a double-layered micro shell for encapsulated drug delivery. *IEEE Trans. Ultrason. Ferroelectr. Freq. Control.* (2004) **51**(7):809-821.

141. ANDERSON JM, SHIVE MS: Biodegradation and biocompatibility of PLA and PLGA microspheres. *Adv. Drug Deliv. Rev.* (1997) **28**(1):5-24.

142. FISHER NG, CHRISTIANSEN JP, KLIBANOV A *et al.*: Influence of microbubble surface charge on capillary transit and myocardial contrast enhancement. *J. Am. College Cardiol.* (2002) **40**(4):811-819.

143. BARBARESE E, HO SY, DARRIGO JS, SIMON RH: Internalization of microbubbles by tumor-cells *in vivo* and *in vitro*. *J. Neuro Oncol.* (1995) **26**(1):25-34.

144. HAMMER DA, APTE SM: Simulation of cell rolling and adhesion on surfaces in shear-flow – general results and analysis of selectin-mediated neutrophil adhesion. *Biophys. J.* (1992) **63**(1):35-57.

145. BRUNK DK, GOETZ DJ, HAMMER DA: Sialyl Lewis(x)/E-selectin-mediate rolling in a cell-free system. *Biophys. J.* (1996) **71**(5):2902-2907.

146. BRUNK DK, HAMMER DA: Quantifying rolling adhesion with a cell-free assay: E-selectin and its carbohydrate ligands. *Biophys. J.* (1997) **72**(6):2820-2833.

147. RODGERS SD, CAMPHAUSEN RT, HAMMER DA: Sialyl Lewis(x)-mediated, PSGL-1-independent rolling adhesion on P-selectin. *Biophys. J.* (2000) **79**(2):694-706.

148. HODGES SR, JENSEN OE: Spreading and peeling dynamics in a model of cell adhesion. *J. Fluid Mech.* (2002) **460**:381-409.

149. PARK EYH, SMITH MJ, STROPP ES *et al.*: Comparison of PSGL-1 microbead and neutrophil rolling: microvillus elongation stabilizes P-selectin bond clusters. *Biophys. J.* (2002) **82**(4):1835-1847.

150. LEI X, LAWRENCE MR, DONG C: Influence of cell deformation on leukocyte rolling adhesion in shear flow. *J. Biomech. Eng.* (1999) **121**(6):636-643.

151. CAO J, DONELL B, DEAVER DR, LAWRENCE MB, DONG C: *In vitro* side-view imaging technique and analysis of human T-leukemic cell adhesion to ICAM-1 in shear flow. *Microvasc. Res.* (1998) **55**(2):124-137.

152. CAO J, USAMI S, DONG C: Development of a side-view chamber for studying cell-surface adhesion under flow conditions. *Ann. Biomed. Eng.* (1997) **25**(3):573-580.

153. ZHAO YH, CHIEN S, SKALAK R: A stochastic-model of leukocyte rolling. *Biophys. J.* (1995) **69**(4):1309-1320.

154. SCHMIDSCHONBEIN GW, SKALAK R, SIMON SI, ENGLER RL: The interaction between leukocytes and endothelium *in vivo*. *Ann. NY Acad. Sci.* (1987) **516**:348-361.

155. ENIOLA AO, HAMMER DA: Characterization of biodegradable drug delivery vehicles with the adhesive properties of leukocytes – II: effect of degradation on targeting activity. *Biomaterials* (2005) **26**(6):661-670.

156. ENIOLA AO, RODGERS SD, HAMMER DA: Characterization of biodegradable drug delivery vehicles with the adhesive properties of leukocytes. *Biomaterials* (2002) **23**(10):2167-2177.

157. LANZA GM, WALLACE KD, SCOTT MJ *et al.*: A novel site-targeted ultrasonic contrast agent with broad biomedical application. *Circulation* (1996) **94**(12):3334-3340.

158. DEMOS SM, ONYUKSEL H, GILBERT J *et al.*: *In vitro* targeting of antibody-conjugated echogenic liposomes for site-specific ultrasonic image enhancement. *J. Pharmaceut. Sci.* (1997) **86**(2):167-171.

159. DEMOS SM, ALKAN-ONYUKSEL H, KANE BJ *et al.*: *In vivo* targeting of acoustically reflective liposomes for intravascular and transvascular ultrasonic enhancement. *J. Am. College Cardiol.* (1999) **33**(3):867-875.

160. LINDNER JR, SONG J, CHRISTIANSEN J *et al.*: Ultrasound assessment of inflammation and renal tissue injury with microbubbles targeted to P-selectin. *Circulation* (2001) **104**(17):2107-2112.

161. LEONG-POI H, KLIBANOV AL, CHRISTIANSEN JP, HUO YQ, LINDNER JR: Development of an angiogenesis-targeted microbubble ultrasound contrast agent. *J. Am. College Cardiol.* (2002) **39**(5):A360.

162. DAVIS CJ, CHRISTIANSEN JP, KLIBANOV AL *et al.*: Microbubbles targeted to endothelial VCAM-1 adhere to atherosclerotic plaques at physiologic shear rates. *Circulation* (2003) **108**(17):624.

163. WELLER GER, VILLANUEVA FS, KLIBANOV AL, WAGNER WR: Modulating targeted adhesion of an ultrasound contrast agent to dysfunctional endothelium. *Ann. Biomed. Eng.* (2002) **30**(8):1012-1019.

164. WELLER GER, LU E, CSIKARI MM *et al.*: Ultrasound imaging of acute cardiac transplant rejection with microbubbles targeted to intercellular adhesion molecule-1. *Circulation* (2003) **108**(2):218-224.

165. WELLER GE, WONG MK, MODZELEWSKI RA *et al.*: Ultrasonic imaging of tumor angiogenesis using contrast microbubbles targeted via the tumor-binding peptide arginine–arginine–leucine. *Cancer Res.* (2005) **65**(2):533-539.

166. HAAG P, FRAUSCHER F, GRADL J *et al.*: Microbubble-enhanced ultrasound to deliver an antisense oligodeoxynucleotide targeting the human androgen receptor into prostate tumours. *J. Steroid Biochem. Mol. Biol.* (2006) **102**(1-5):103-113.

167. BEKEREDJIAN R, KUECHERER HF, KROLL RD, KATUS HA, HARDT SE: Ultrasound-targeted microbubble destruction augments proteins delivery into testes. *Urology* (2007) **69**(2):386-389.

168. TAYLOR SL, RAHIM AA, BUSH NL, BARNBER JC, PORTER CD: Targeted retroviral gene delivery using ultrasound. *J. Gene Med.* (2007) **9**(2):77-87.

169. NEWMAN CMH, BETTINGER T: Gene therapy progress and prospects: ultrasound for gene transfer. *Gene Ther.* (2007) **14**(6):465-475.

170. RAHIM AA, TAYLOR SL, BUSH NL *et al.*: Spatial and acoustic pressure dependence of microbubble-mediated gene delivery targeted using focused ultrasound. *J. Gene Med.* (2006) **8**(11):1347-1357.

171. WANG XH, LIANG HD, DONG BW, LU QL, BLOMLEY MJK: Gene transfer with microbubble ultrasound and plasmid DNA into skeletal muscle of mice: comparison between commercially available microbubble contrast agents. *Radiology* (2005) **237**(1):224-229.

172. JAYAWEERA AR, EDWARDS N, GLASHEEN WP *et al.*: *In-vivo* myocardial kinetics of air-filled albumin microbubbles during myocardial contrast

echocardiography – comparison with radiolabeled red-blood-cells. *Circ. Res.* (1994) **74**(6):1157-1165.

173. FIRRELL JC, LIPOWSKY HH: Leukocyte margination and deformation in mesenteric venules of rat. *Am. J. Physiol.* (1989) **256**(6):H1667-H1674.
174. TARDY I, POCHON S, THERAULAZ M, NANJAPPAN P, SCHNEIDER M: *In vivo* ultrasound imaging of thrombi using a target-specific contrast agent. *Acad. Radiol.* (2002) **9**:S294-S296.
175. VILLANUEVA FS, ABRAHAM JA, SCHREINER GF *et al.*: Myocardial contrast echocardiography can be used to assess the microvascular response to vascular endothelial growth factor-121. *Circulation* (2002) **105**(6):759-765.
176. KLIBANOV AL, RASCHE PT, HUGHES MS *et al.*: Detection of individual microbubbles of an ultrasound contrast agent: fundamental and pulse inversion imaging. *Acad. Radiol.* (2002) **9**:S279-S281.
177. SCHUMANN PA, CHRISTIANSEN JP, QUIGLEY RM *et al.*: Targeted-microbubble binding selectively to GPIIb IIIa receptors of platelet thrombi. *Investig. Radiol.* (2002) **37**(11):587-593.
178. KIM DH, KLIBANOV AL, NEEDHAM D: The influence of tiered layers of surface-grafted poly(ethylene glycol) on receptor–ligand-mediated adhesion between phospholipid monolayer-stabilized microbubbles and coated class beads. *Langmuir* (2000) **16**(6):2808-2817.
- **Quantified advantages of spacer arms for adhesion.**

179. LONGO G, SZLEIFER I: Ligand–receptor interactions in tethered polymer layers. *Langmuir* (2005) **21**(24):11342-11351.
180. LIN JJ, SILAS JA, BERMUDEZ H *et al.*: The effect of polymer chain length and surface density on the adhesiveness of functionalized polymersomes. *Langmuir* (2004) **20**(13):5493-5500.
181. TAKALKAR AM, KLIBANOV AL, RYCHAK JJ, LINDNER JR, LEY K: Binding and detachment dynamics of microbubbles targeted to P-selectin under controlled shear flow. *J. Control. Rel.* (2004) **96**(3):473-482.
182. HAM ASW, GOETZ DJ, KLIBANOV AL, LAWRENCE MB: Microparticle adhesive dynamics and rolling mediated by selectin-specific antibodies under flow. *Biotechnol. Bioeng.* (2007) **96**(3):596-607.
183. KLIBANOV AL, RYCHAK JJ, YANG WC *et al.*: Targeted ultrasound contrast agent for molecular imaging of inflammation in high-shear flow. *Contrast Media Mol. Imaging* (2006) **1**(6):259-266.
184. FOWLKES JB, GARDNER EA, IVEY JA, CARSON PL: The role of acoustic radiation force in contrast enhancement techniques using bubble-based ultrasound contrast agents. *J. Acoust. Soc. Am.* (1993) **93**:2348.
- **Showed the ability of acoustic radiation force to direct microbubbles.**

185. DAYTON P, KLIBANOV A, BRANDENBURGER G, FERRARA K: Acoustic radiation force *in vivo*: a mechanism to assist targeting of microbubbles. *Ultrasound Med. Biol.* (1999) **25**(8):1195-1201.
- **Showed potential of radiation force for assisting targeting.**

186. ZHAO S, BORDEN M, BLOCH S *et al.*: Radiation force assisted targeting facilitates ultrasonic molecular imaging. *Mol. Imaging* (2004) **3**:1-14.
187. RYCHAK JJ, KLIBANOV AL, HOSSACK JA: Acoustic radiation force enhances targeted delivery of ultrasound contrast microbubbles: *in vitro* verification. *IEEE Trans. Ultrason. Ferroelectr. Freq. Control.* (2005) **52**(3):421-433.
188. LUM AFH, BORDEN MA, DAYTON PA *et al.*: Ultrasound radiation force enables targeted deposition of model drug carriers loaded on microbubbles. *J. Control. Rel.* (2006) **111**(1-2):128-134.
189. BORDEN MA, SARANTOS MR, STIEGER SM *et al.*: Ultrasound radiation force modulates ligand availability on targeted contrast agents. *Mol. Imaging* (2006) **5**(3):139-147.
190. DAYTON PA, ZHAO SK, BLOCH SH *et al.*: Application of ultrasound to selectively localize nanodroplets for targeted imaging and therapy. *Mol. Imaging* (2006) **5**(3):160-174.
191. RYCHAK JJ, LINDNER JR, LEY K, KLIBANOV AL: Deformable gas-filled microbubbles targeted to P-selectin. *J. Control. Rel.* (2006) **114**(3):288-299.
192. MEDWIN H: Counting bubbles acoustically – review. *Ultrasonics* (1977) **15**(1):7-13.
193. LEONG-POI H, SONG J, RIM SJ *et al.*: Influence of microbubble shell properties on ultrasound signal: implications for low-power perfusion imaging. *J. Am. Soc. Echocardiogr.* (2002) **15**(10):1269-1276.
194. RAYLEIGH L: On the pressure developed in a liquid during the collapse of a spherical cavity. *Phil. Mag.* (1917) **34**:94-98.
195. PLESSET MS: The dynamics of cavitation bubbles. *J. Appl. Mech. Trans. Asme* (1949) **16**(3):277-282.
196. CULP WC, PORTER TR, LOWERY J *et al.*: Intracranial clot lysis with intravenous microbubbles and transcranial ultrasound in swine. *Stroke* (2004) **35**(10):2407-2411.
197. LINDNER JR: Evolving applications for contrast ultrasound. *Am. J. Cardiol.* (2002) 90(10A):J72-J80.
198. MIYOSHI N, SOSTARIC JZ, RIESZ P: Correlation between sonochemistry of surfactant solutions and human leukemia cell killing by ultrasound and porphyrins. *Free Radic. Biol. Med.* (2003) **34**(6):710-719.
199. ROSENTHAL I, SOSTARIC JZ, RIESZ P: Sonodynamic therapy – a review of the synergistic effects of drugs and ultrasound. *Ultrasonics Sonochem.* (2004) **11**(6):349-363.
200. SONG J, CHAPPELL JC, QI M *et al.*: Influence of injection site, microvascular pressure and ultrasound variables on microbubble-mediated delivery of microspheres to muscle. *J. Am. College Cardiol.* (2002) **39**(4):726-731.
201. BLAKE JR, GIBSON DC: Cavitation bubbles near boundaries. *Annu. Rev. Fluid Mech.* (1987) **19**:99-123.
202. BLAKE JR, HOOTON MC, ROBINSON PB, TONG RP: Collapsing cavities, toroidal bubbles and jet impact. *Phil. Trans. Roy. Soc. Lond. Series A Math. Phys. Eng. Sci* (1997) **355**(1724):537-550.
203. BLAKE JR, KEEN GS, TONG RP, WILSON M: Acoustic cavitation: the fluid dynamics of non-spherical bubbles. *Phil. Trans. Roy. Soc. Lond. Series A Math. Phys. Eng. Sci.* (1999) **357**(1751):251-267.
204. BLAKE JR, TAIB BB, DOHERTY G: Transient cavities near boundaries. 1. Rigid boundary. *J. Fluid Mech.* (1986) **170**:479-497.

205. BLAKE JR, TOMITA Y, TONG RP: The art, craft and science of modelling jet impact in a collapsing cavitation bubble. *Appl. Scientific Res.* (1998) **58**(1-4):77-90.

206. BOURNE NK: On the collapse of cavities. *Shock Waves* (2002) **11**(6):447-455.

207. SZERI AJ, STOREY BD, PEARSON A, BLAKE JR: Heat and mass transfer during the violent collapse of nonspherical bubbles. *Phys. Fluids* (2003) **15**(9):2576-2586.

208. BRUJAN EA, KEEN GS, VOGEL A, BLAKE JR: The final stage of the collapse of a cavitation bubble close to a rigid boundary. *Phys. Fluids* (2002) **14**(1):85-92.

209. CHRISTIANSEN JP, FRENCH BA, KLIBANOV AL, KAUL S, LINDNER JR: Targeted tissue transfection with ultrasound destruction of plasmid-bearing cationic microbubbles. *Ultrasound Med. Biol.* (2003) **29**(12):1759-1767.

210. BORDEN MA, KRUSE DE, CASKEY CF *et al.*: Influence of lipid shell physicochemical properties on ultrasound-induced microbubble destruction. *IEEE Trans. Ultrason. Ferroelectr. Freq. Control.* (2005) **52**(11):1992-2002.

211. PORTER TR, IVERSEN PL, LI SP, XIE F: Interaction of diagnostic ultrasound with synthetic oligonucleotide-labeled perfluorocarbon-exposed sonicated dextrose albumin microbubbles. *J. Ultrasound Med.* (1996) **15**(8):577-584.

212. YE T, BULL JL: Direct numerical simulations of micro-bubble expansion in gas embolotherapy. *J. Biomech. Eng.* (2004) **126**(6):745-759.

• **Contains details of a rigid vessel model whose results are shown in Figure 2.**

213. YE T, BULL JL: Microbubble expansion in a flexible tube. *J. Biomech. Eng.* (2006) **128**(4):554-563.

• **Contains details of a flexible vessel model whose results are shown in Figure 3.**

214. QIN SP, FERRARA KW: Acoustic response of compliable microvessels containing ultrasound contrast agents. *Phys. Med. Biol.* (2006) **51**(20):5065-5088.

215. QIN SP, HU YT, JIANG Q: Oscillatory interaction between bubbles and confining microvessels and its implications on clinical vascular injuries of shock-wave lithotripsy. *IEEE Trans. Ultrason. Ferroelectr. Freq. Control.* (2006) **53**(7):1322-1329.

216. CHEN SY, SHOHET RV, BEKEREDJIAN R, FRENKEL P, GRAYBURN PA: Optimization of ultrasound parameters for cardiac gene delivery of adenoviral or plasmid deoxyribonucleic acid by ultrasound-targeted microbubble destruction. *J. Am. College Cardiol.* (2003) **42**(2):301-308.

217. MUKHERJEE D, WONG J, GRIFFIN B *et al.*: Ten-fold augmentation of endothelial uptake of vascular endothelial growth factor with ultrasound after systemic administration. *J. Am. College Cardiol.* (2000) **35**(6):1678-1686.

218. KINOSHITA M, HYNYNEN K: Intracellular delivery of Bak BH3 peptide by microbubble-enhanced ultrasound. *Pharm. Res.* (2005) **22**(5):716-720.

219. ZHAO YZ, LIANG HD, MEI XG, HALLIWELL M: Preparation, characterization and *in vivo* observation of phospholipid-based gas-filled microbubbles containing hirudin. *Ultrasound Med. Biol.* (2005) **31**(9):1237-1243.

220. MEAIRS S, ALONSO A: Ultrasound, microbubbles and the blood–brain barrier. *Prog. Biophys. Mol. Biol.* (2007) **93**(1-3):354-362.

221. HYNYNEN K: Focused ultrasound for blood–brain disruption and delivery of therapeutic molecules into the brain. *Expert Opin. Drug Deliv.* (2007) **4**(1):27-35.

• **Review of focused ultrasound for BBB disruption.**

222. HILLS BA, JAMES PB: Microbubble damage to the blood–brain-barrier – relevance to decompression-sickness. *Undersea Biomed. Res.* (1991) **18**(2):111-116.

223. VYKHODTSEVA NI, HYNYNEN K, DAMIANOU C: Histologic effects of high-intensity pulsed ultrasound exposure with subharmonic emission in rabbit brain *in vivo*. *Ultrasound Med. Biol.* (1995) **21**(7):969-979.

224. HYNYNEN K, MCDANNOLD N, VYKHODTSEVA N, JOLESZ FA: Noninvasive MR imaging-guided focal opening of the blood-brain barrier in rabbits. *Radiology* (2001) **220**(3):640-646.

• **Demonstrated that focused ultrasound in the presence of microbubble contrast agent can be used to consistently open the BBB.**

225. HYNYNEN K, MCDANNOLD N, MARTIN H, JOLESZ FA, VYKHODTSEVA N: The threshold for brain damage in rabbits induced by bursts of ultrasound in the presence of an ultrasound contrast agent (Optison (R)). *Ultrasound Med. Biol.* (2003) **29**(3):473-481.

226. SCHLACHETZKI F, HOLSCHER T, KOCH HJ *et al.*: Observation on the integrity of the blood–brain barrier after microbubble destruction by diagnostic transcranial color-coded sonography. *J. Ultrasound Med.* (2002) **21**(4):419-429.

227. SHEIKOV N, MCDANNOLD N, VYKHODTSEVA N, JOLESZ F, HYNYNEN K: Cellular mechanisms of the blood–brain barrier opening induced by ultrasound in presence of microbubbles. *Ultrasound Med. Biol.* (2004) **30**(7):979-989.

228. MCDANNOLD N, VYKHODTSEVA N, JOLESZ FA, HYNYNEN K: MRI investigation of the threshold for thermally induced blood–brain barrier disruption and brain tissue damage in the rabbit brain. *Magn. Reson. Med.* (2004) **51**(5):913-923.

229. HYNYNEN K, MCDANNOLD N, SHEIKOV NA, JOLESZ FA, VYKHODTSEVA N: Local and reversible blood–brain barrier disruption by noninvasive focused ultrasound at frequencies suitable for *trans*-skull sonications. *Neuroimage* (2005) **24**(1):12-20.

230. MCDANNOLD N, VYKHODTSEVA N, RAYMOND S, JOLESZ FA, HYNYNEN K: MRI-guided targeted blood–brain barrier disruption with focused ultrasound: histological findings in rabbits. *Ultrasound Med. Biol.* (2005) **31**(11):1527-1537.

231. MCDANNOLD N, VYKHODTSEVA N, HYNYNEN K: Targeted disruption of the blood–brain barrier with focused ultrasound: association with cavitation activity. *Phys. Med. Biol.* (2006) **51**(4):793-807.

232. YIN XT, HYNYNEN K: A numerical study of transcranial focused ultrasound beam propagation at low frequency. *Phys. Med. Biol.* (2005) **50**(8):1821-1836.

233. SHEIKOV N, MCDANNOLD N, JOLESZ F *et al.*: Brain arterioles show more active vesicular transport of

blood-borne tracer molecules than capillaries and venules after focused ultrasound-evoked opening of the blood–brain barrier. *Ultrasound Med. Biol.* (2006) **32**(9):1399-1409.

234. HYNYNEN K, MCDANNOLD N, VYKHODTSEVA N *et al.*: Focal disruption of the blood–brain barrier due to 260-kHz ultrasound bursts: a method for molecular imaging and targeted drug delivery. *J. Neurosurg.* (2006) **105**(3):445-454.
235. KINOSHITA M, MCDANNOLD N, JOLESZ FA, HYNYNEN K: Noninvasive localized delivery of herceptin to the mouse brain by MRI-guided focused ultrasound-induced blood–brain barrier disruption. *Proc. Natl. Acad. Sci. USA* (2006) **103**(31):11719-11723.
236. KINOSHITA M, MCDANNOLD N, JOLESZ FA, HYNYNEN K: Targeted delivery of antibodies through the blood–brain barrier by MRI-guided focused ultrasound. *Biochem. Biophys. Res. Commun.* (2006) **340**(4):1085-1090.
237. MCDANNOLD N, VYKHODTSEVA N, HYNYNEN K: Use of ultrasound pulses combined with definity for targeted blood–brain barrier disruption: a feasibility study. *Ultrasound Med. Biol.* (2007) **33**(4):584-590.
238. CHOI JJ, PERNOT M, SMALL SA, KONOFAGOU EE: Noninvasive, transcranial and localized opening of the blood–brain barrier using focused ultrasound in mice. *Ultrasound Med. Biol.* (2007) **33**(1):95-104.
239. COUSSIOS CC, FARNY CH, TER HAAR G, ROY RA: Role of acoustic cavitation in the delivery and monitoring of cancer treatment by high-intensity focused ultrasound (HIFU). *Intern. J. Hyperthermia* (2007) **23**(2):105-120.
240. YANAGISAWA K, MORIYASU F, MIYAHARA T, YUKI M, IIJIMA H: Phagocytosis of ultrasound contrast agent microbubbles by Kupffer cells. *Ultrasound Med. Biol.* (2007) **33**(2):318-325.
241. DENNIS MS, JIN HK, DUGGER D *et al.*: Imaging tumors with an albumin-binding Fab, a novel tumor-targeting agent. *Cancer Res.* (2007) **67**(1):254-261.
242. KINDBERG GM, TOLLESHAUG H, ROOS N, SKOTLAND T: Hepatic clearance of Sonazoid perfluorobutane microbubbles by Kupffer cells does not reduce the ability of liver to phagocytose or degrade albumin microspheres. *Cell Tissue Res.* (2003) **312**(1):49-54.
243. CORREAS JM, MEUTER AR, SINGLAS E *et al.*: Human pharmacokinetics of a perfluorocarbon ultrasound contrast agent evaluated with gas chromatography. *Ultrasound Med. Biol.* (2001) **27**(4):565-570.

Affiliation

Joseph L Bull PhD
The University of Michigan,
Departments of Biomedical Engineering and Surgery, 2142 Lurie Biomedical Engineering Building, 1107 Beal Avenue,
Ann Arbor, MI 48109, USA
Tel: +1 734 647 5395; Fax: +1 734 647 4834;
E-mail: joebull@umich.edu